Mechanism of groundwater inrush hazard caused by solution mining in multilayer rock salt mine area: a case study in Tongbai County, China

Bin Zeng[1*], Tingting Shi[2], Zhihua Chen[1], Liu Xiang[3], Shaopeng Xiang[4], Muyi Yang[1]

[1]. School of Environmental Studies, China University of Geosciences, Wuhan 430074, Hubei, P.R.China.

[2]. Three Gorges Research Center for Geo-Hazard, Ministry of Education, Wuhan 430074, Hubei, P.R.China.

[3]. Department of Geological Engineering, Hubei Land Resources Vocational College. Wuhan 430074, P.R.China.

[4]. Hydrological Engineering Environment Technology Consulting Co. Ltd. Wuhan 430074, P.R.China.

Corresponding author: Bin Zeng, Ph.D.

Affiliation: School of Environmental Studies, China University of Geosciences.

Affiliation address: No. 388 Lumo Road, Wuhan, Hubei, 430074, P.R. China.

Email: zengbin_19@126.com. Tel: 86-27-67883473. Fax: 86-27-87436235.

ABSTRACT

The solution mining of salt mineral resources may contaminate groundwater and lead to water inrush out of the ground due to brine leakage. Taking a serious groundwater inrush hazard in a large salt mining area with three different types of ore beds which are trona (trisodium hydrogendicarbonate dihydrate, also sodium sesquicarbonate dihydrate, $Na_2CO_3 \cdot NaHCO_3 \cdot 2H_2O$, is a non-marine evaporite mineral), glauber (sodium sulfate, is the inorganic compound with formula Na_2SO_4 as well as several related hydrates) and gypsum (a soft sulfate mineral composed of calcium sulfate dihydrate, with the chemical formula $CaSO_4 \cdot 2H_2O$) in Tongbai County of China as an example, this paper mainly aims to analyse the source and channel of the inrush water. Based on the understanding of geological and hydrogeological conditions, the study obtained hydrochemical data of groundwater at different points and depths first; and then analysed the pollution source and pollutant component from single or mixed brines by both physical-chemical reaction principle analysis and hydrogeochemistry simulation method; finally possible leakage brine conducting channel to the ground had been discussed from both geological and artificial aspects. The results reveal that the brine from the trona mine is the major pollution source; the fissure zone in NW-SE direction controlled by the geological structure provides the main channels for the leakage brine to flow into the aquifer around the water inrush regions, and a large number of waste gypsum exploration boreholes are the channels that supply the polluted groundwater inrush out of the ground. The research can offer a valuable reference for avoiding and assessing groundwater inrush hazard in similar rock salt mining area, which is advantageous for both groundwater quality protection and resident health.

1. **Introduction**

Solution mining is commonly used in salt mine exploitation, as salts are soluble in water. In this method, high-pressure and -temperature water with low salinity is injected into a mineral deposit through production wells to dissolve the mineral salts. After being transported out of the wells, the soluble salt is purified and further processed. However, the high-pressure and -temperature water used in this process not only dissolves minerals but also may cause fracture of strata, which usually results in hazards such as brine leakage or groundwater inrush. So that underground drinking water for residents is normally polluted after the groundwater inrush hazard, and make threaten to the health of local people.

Many scholars (Clark and Fritz, 1997; Liu et al., 2015; Wu et al., 2016) have studied the case of groundwater inrush hazards in both coal and metal mines, and some adopted methods are as follow: the use of water level/temperature criterion (Yuan and Gui, 2005; Ma and Qian, 2014), stochastic simulation (Fernandez-Galvez et al., 2007), numerical simulation (Liu et al., 2009; Kang et al., 2012; Shao et al., 2013; Houben, et al., 2017), water chemical analysis (Robins, 2002; Fernandez et al., 2005; Hu et al., 2010; Cobbina et al., 2015; Lee et al., 2016; LeDoux et al., 2016) (isotope analysis, water quality type correlation analysis), multivariate statistics (Chen and Li, 2009; Lu, 2012) (discriminant analysis, clustering analysis), fractional advection dispersion equations (Ramadas et al., 2015) and nonlinear analysis (Hao et al., 2010; Gao, 2012) (fuzzy mathematics, grey correlation analysis, etc.).

55   However, due to the particularity of mining method (solution mining) and complex chemical-physical

56   reactions during mining process (under high-pressure and -temperature), research about solution

57   mining is more focusing on mining techniques (Jiang and Jiang, 2004; Kotwica, 2008; Namin et al.,

58   2009), mining cavity stability analysis and sinkhole problem (Staudtmeister and Rokahr, 1997;

59   Bonetto et al., 2008; Ezersky et al., 2009; Goldscheider and Bechtel, 2009; Closson and Abou Karaki,

60   2009; Vigna et al., 2010; Frumkin et al., 2011; Ezersky and Frumkin, 2013; Qiu, 2011; Blachowski et

61   al., 2014), and geohazards especially in karst area due to human-induced underground caves (Waltham

62   and Fookes 2003; Parise and Gunn 2007; Zhou and Beck 2011; Parise and Lollino 2011; Lollino et al.,

63   2013; Gutierrez et al., 2014; Parise et al., 2015), but rarely on the source and channel analysis of

64   inrush water in solution mining accident.

65   The studied rock salt mine area is located in Tongbai County of Henan province in China. This

66   mine area has the second largest trona reserves worldwide, while its glauber salt reserves reaches 45

67   million tons. Since trona and glauber salt had been put into production in 1990 with single and double

68   well convection mining as their main producing method, from June 2011 to May 2013, five inrush

69   points appeared in Anpeng Town of Tongbai County. Among these five inrush points, four (Y1~Y4)

70   were long-term (more than 2 years) inrush points with stable discharge, while one (Y-5) was a sudden

71   inrush point (as shown in Fig. 1 and Fig. 3). On 1 February, 2013, almost 200 m^3 of mud and sediment

72   erupted out of the ground at Y-5 point. The area of inrush point was almost 4 m^2; the average water

73 inflow was 20-30 m^3/d while the largest inflow reached 20 d, and the water inrush lasted for

74 approximately 3 months. During the Y-5 inrush accident, according to the field investigation, a trona

75 production well named "S02", which is 200 m away from the inrush point, was broken at the depth of

76 234 m for a long period of time, and it was repaired on 15 March, 2013. During the whole water inrush

77 process, the inrush groundwater led to the phenomenon of salinization at the house bottom in many

78 villagers, and made water in many resident wells undrinkable any more.

79   Since the groundwater inrush hazard involving a wide range and the inrush source is quite hard to

80 distinguish due to the multi-layer distribution of different ore body and complex of inrush water

81 component. Therefore, in order to put forward a targeted treatment program to stop the water inrush as

82 soon as possible, and mitigate the groundwater pollution in research region, the source and channel of

83 inrush water were taken as the research emphasis in this paper. Furthermore, the research can offer a

84 valuable reference for avoiding and assessing groundwater inrush hazard in similar rock salt mining

85 area, which is advantageous for both groundwater quality protection and resident health.

86 **2. Geological and hydrogeological setting**

87 *2.1. Geological conditions*

88   The mining area is located in northwest of Tongbai County. The landscape is characterized by

89 hollows and ridges, and has an elevation ranging between 140 and 200 m. Information about the strata,

90 lithology, aquifer, and position of different ore beds in research area (Shi et al., 2013) are shown in Fig.

91

92   According to the field investigation, in the mining area, some buried faults develop in the

93   Hetaoyuan Formation, but these faults have only small effect on the ore bed because they are either

94   outside of the ore bed or distribute in a limited area.

95   *2.2. Hydrogeological conditions*

96   The groundwater in the mining area can be divided into pore water in the loose rock mass and

97   bedrock fissure water according to lithology and hydrogeological features. In the upper part of

98   Liaozhuang Formation, mudstone interbedded with gypsum is considered as the aquiclude. The

99   shallow aquifer is an unconsolidated pore water aquifer located above the aquiclude, while the deep

100   aquifer is a bedrock fissure aquifer located under the aquiclude. The water inflow of a single well with

101   poor water content is approximately 10 m^3/d, while it can reach 1000-2000 m^3/d with rich water

102   content. The annual variation of groundwater level is 2-4 m, while the depth is stable at 2.3-4 m.

103   Residents in Anpeng Town take groundwater as source of drinking water, which comes from the well

104   and belongs to porous aquifer.

105   As shown in Fig. 3, gypsum mainly exists on the top of the Liaozhuang Formation, glauber salt

106   exists in the third member of the Hetaoyuan Formation, and trona exists at the bottom of the second

107   member of the Hetaoyuan Formation and on top of the first member of the Hetaoyuan Formation. The

108   surrounding rocks of every mineral layer include mudstone, shale, psammitic rock and dolomite,

109   which have sufficient thickness and good water-resistance ability. Therefore, the effect of groundwater

110   on the mineral deposit is minimal in the mining area.

111   *2.3 Distribution and characteristics of the ore body*

112   The three ore bodies overlap in plane distribution, as shown in Fig. 3. The vertical distribution of

113   ore bodies from deep to shallow is trona (buried depth: 1560.92-2929.53 m), glauber salt (buried

114   depth: 1003.66-1397.5 m) and gypsum (buried depth: 134-338 m). Trona and glauber salt are at least

115   250 m apart from each other vertically.

116   Trona has 11 horizontal layers, with an average thickness of 2 m. The chemical composition of

117   trona is mainly $NaHCO_3$ (average of 77.06%) and Na_2CO_3 (average of 16.33%) (Wang, 1987).

118   Glauber salt has 4 layers, with an average thickness of 8.93m. The dip angle of ore bed layer is within

119   10°. The average mineral grade is 60.14%. The main composition of glauber salt is Na_2SO_4 (>90%),

120   and with a small amount of NaCl.

121   **3. Methods**

122   Based on the field investigation result, the chemical characteristic analysis of inrush water in

123   different sites and time, and analysis of physical and chemical reaction principle for different brines,

124   combined with PHREEQC simulation method were adopted to judge the source of inrush water.

125   *3.1. Sampling and test*

126   The 5 groundwater inrush points (Y1~Y5) and some shallow groundwater points (resident wells:

127 SY1~SY6) nearby the accident site were chosen as groundwater quality sampling points, as shown in

128 Fig. 3. Water from each point was sampled on 9 March, 2013.

129 Water samples were filtered by 0.45 μm millipore filtration membrane in the field, and then filled

130 with a polyethylene bottle which had been soaked in acid and washed with de ionized water. Filtered

131 water samples were acidized until pH<2 by addition of ultra-pure HNO_3^- for the determination of

132 cation; water samples for the determination of anion would not be treated.

133 Elements tested in laboratory include 26 cations (K^+, Na^+, Ca^{2+}, Mg^{2+}, Sr^{2+}, etc.) and 5 anions (F^-,

134 Cl^-, NO_3^-, SO_4^{2-}, NO_2^-). The instrument for the determination of cation is inductively coupled plasma

135 atomic emission spectrometer (Agilent ICP-OES 5100), while the minimum detection limit is

136 0.0001mg/L; the instrument for the determination of anion is ion chromatograph (ICS-1100), while

137 the minimum detection limit is 0.001 mg/L. CO_3^{2-} and HCO_3^- were tested according to "Groundwater

138 quality test method: Determination of carbonate and bicarbonate by hydroxide titration (DZ/T

139 0064.49-93)", while the minimum detection limit is 0.01 mg/L.

140 In addition, from March to April 2013, at Y-5 and Y-3 points, three water quality automatic

141 recorders (Levelogger gold, Canada) were arranged for the inrush water monitoring. Monitoring

142 indicators were temperature, water level and electrical conductivity. The monitoring purpose was to

143 master the inrush water quality during the whole accident, especially in the process of well reparation.

3.2. Analysis on physical and chemical reaction principle in different brine mixing conditions

144

145   During the accident, the leakage brine of trona (2000 m below the ground) or glauber salt mine

146   (1000 m below the ground) might flow through the gypsum deposit (200-400 m below the ground,

147   comprising primarily $CaSO_4$) and caused physical and chemical reactions while inrush out of the

148   ground. So the formation of inrush water chemistry component might be by glauber brine, or trona brine,

149   or a mixture of the two brines flowed through the gypsum layer with physical and chemical reaction. To

150   provide the basis for further analysis of the inrush water source, the physical solubility of gypsum, the

151   reaction when glauber salt brine, trona brine, mixture of trona and glauber salt brine flow through the

152   gypsum deposits were analysed.

153   *3.2.1. The physical solubility of gypsum ($CaSO_4$)*

154   Gypsum is slightly soluble; when in water, its acidity is apparent. Eq. (1) gives the dissolution rate

155   equation of gypsum in water:

156
$$R_{Gypsum} = k_1 \times \frac{A_g}{V}(1 - (\frac{IAP}{K})_{Gypsum}) \tag{1}$$

157   R_{Gypsum}: the dissolution rate of gypsum; k_1: rate constant; A_g: the surface area of gypsum; V: the

158   liquid volume in contact with the gypsum surface; IAP: the product of ion activity; K: ion solubility

159   product.

160    $(\frac{IAP}{K})_{Gypsum}$ is affected by the temperature; thus, it is the same as R_{Gypsun}.

161   The solubility of gypsum in water reaches a maximum of 0.2097 g/100 g at 40℃. The solubility

162   decreases when the temperature is below or above 40℃, the content of SO_4^{2-} and Ca^{2+} obtained by

163   physical dissolution is very low.

164   *3.2.2. Gypsum (CaSO₄) dissolved by glauber salt brine (Na₂SO₄)*

165   Equations (2) and (3) show the reactions of Na_2SO_4 and $CaSO_4$ with water.

$$Na_2SO_4 \leftrightharpoons 2Na^+ + SO_4^{2-} \tag{2}$$

$$CaSO_4 \leftrightharpoons Ca^{2+} + SO_4^{2-} \tag{3}$$
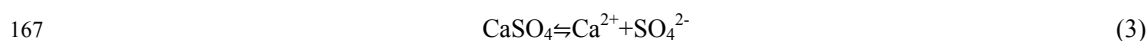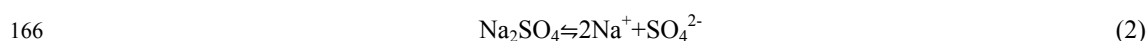
168   Due to the common-ion effect, the solubility of the electrolyte will decrease when a strong

169   electrolyte with the same ion is put into an electrolyte-saturated solution. Thus, the solubility of gypsum

170   will be reduced when glauber salt brine flows through and dissolves the gypsum deposits, the gypsum

171   will even harder to be dissolved in this situation. So if glauber salt brine flows through the gypsum

172   deposits, the brine characteristic would not be changed apparently.

173   *3.2.3. The reaction of trona brine or a mixture of trona and glauber salt brine with gypsum*

174   The HCO_3^- and CO_3^{2-} contents in mixed brine or trona brine are very high and so are the solution

175   alkalinity and pH. If the reaction kinetics is not taking into account, the pH has little influence on the

176   dissolution of gypsum (Yang, 2003; Xu and Li, 2011). The reaction occurs when the brine with high

177   concentrations of HCO_3^- and CO_3^{2-} flows through the gypsum deposits. The main chemical reactions

178   are:

179 $$Na_2CO_3+CaSO_4 \leftrightarrows Na_2SO_4+CaCO_3\downarrow \qquad\qquad (4)$$

180 $$2NaHCO_3+CaSO_4 \leftrightarrows Ca(OH)_2+ \ Na_2SO_4+2CO_2\uparrow \qquad\qquad (5)$$
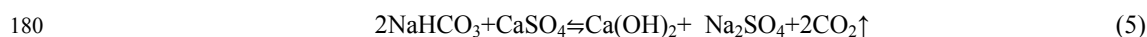
181   In Eq. (4), $CaSO_4$ is slightly soluble, while $CaCO_3$ is insoluble. The reaction easily occurs when

182 insoluble substance is produced by slight soluble substance, the ionic equation is:

183 $$CO_3^{2-}+CaSO_4 \cdot 2H_2O \leftrightarrows SO_4^{2-}+CaCO_3\downarrow+2H_2O \qquad\qquad (6)$$
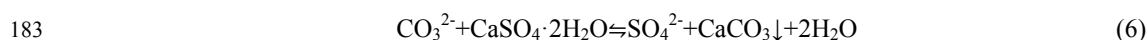
184   The Gibbs Free Energy ($\triangle G$) is -22.7 kJ/mol under the standard state. When $\triangle G$ is negative, the

185 reaction, which is endothermic, happens freely. The reaction is faster at higher temperatures. Eq. (5)

186 shows that $\triangle G$ is 2102 kJ/mol under the standard state. When $\triangle G$ is positive, the reaction will not

187 happen freely.

188   Thus, the reaction shown in Eq. (5) won't occur, the chemical reaction will still proceed as shown

189 in Eq. (4), when trona brine or mixed brine flow through gypsum deposits.

190 *3.2.4. The carbonate equilibrium effect during the reaction of different brine*

191   The carbonate equilibrium that exists in trona brine or mixed brine is affected by pH. The

192 carbonate in groundwater exists in three forms: free carbonic acid, bicarbonate and carbonic acid.

193   In trona brine (pH>10), concentration of HCO_3^- is 5-20 times the concentration of CO_3^{2-}, and

194 CO_3^{2-} in the brine is dominant in this case. When trona brine flows through the gypsum, $CaSO_4$ reacts

195 with CO_3^{2-} and $CaCO_3$ precipitation is generated. If the concentration of CO_3^{2-} in brine decreases, the

196 reversible reaction will take place and drive the equilibrium to the right. Thus, the reverse reaction

197 will occur when trona brine flows through the gypsum.

$$CO_3^{2-}+CaSO_4 \rightleftharpoons SO_4^{2-}+CaCO_3\downarrow \qquad (7)$$

$$HCO_3^- \rightleftharpoons H^+ + CO_3^{2-} \qquad (8)$$
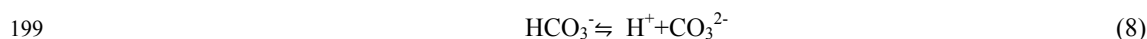
200 The circular reactions as shown in Eqs. (7) and (8) will occur when mixed brine flows through the

201 gypsum because of the similar properties with trona brine. Thus, taking the carbonate equilibrium

202 effect into account, the concentration of HCO_3^- and CO_3^{2-} will decrease, while SO_4^{2-} increases after

203 $CaCO_3$ precipitation was generated.

204 ### 3.3. Simulation of groundwater inrush source

205 For further quantitative analysis of inrush water source and component, the international

206 hydrological and geochemical simulation software PHREEQC was adopted to simulate the water rock

207 interaction. PHREEQC (~~DzavidL,~~ Parkurst and C.A.J. Appelo, 1999) was exploited by USGS, it can

208 calculate the geochemical action under temperature range of 0~300 degrees (Wei, 2010).

209 Based on the deduction that the main water inrush source around Anpeng town was trona leakage

210 brine, the research used the simulation method PHREEQC combined with the possible channel of

211 inrush water to establish a conceptual model and then carried out hydrogeochemical simulation of the

212 water-rock interaction. Subsequently, the research quantified the mixed ratio of inrush groundwater

213 and shallow groundwater around Anpeng town, which can better verify the source of inrush water.

214   *3.3.1. Conceptual model*

215   Around Anpeng town, the trona leakage brine flowed through the specified mineral assemblages

216   and mixed with shallow groundwater in different proportions.

217   *3.3.2. Initial data input*

218   The parameters of trona brine were taken from enterprise's production testing data; the parameters

219   of shallow groundwater were taken from the same aquifer but outside the study area, which can

220   basically represent the groundwater background values. The specific parameters are shown in Table 1:

221   *3.3.3. Setting of stratum and mineral*

222   The formations from the bottom to top during the process of the leakage brine flowing into the

223   shallow groundwater and then pouring out of the ground were as follows: third member of the

224   Hetaoyuan Formation of Paleogene, Liaozhuang Formation, Fenghuang Formation of Neogene and

225   Quaternary. To simplify the mining area, according to the thickness of rock stratum and the proportion

226   of mineral composition,it can be assumed that the layer through which the trona brine flowed contains

227   Ca-montmorillonite, kaolinite, gypsum, potash feldspar and potash mica.

228   The main ingredients are as follow: Kaolinite: $Al_4[Si_4O_{10}](OH)_8$; Gypsum: $CaSO_4 \cdot 2H_2O$;

229   Ca-montmorillonite: $(Na,Ca)_{0.33}(Al,Mg)_2[Si_4O_{10}](OH)_2 \cdot nH_2O$; Dolomite: $CaCO_3$; Potash feldspar: K

230    $[AlSi_3O_8]$; Poash mica: aluminum silicate as K, Al, Mg, Fe and Li.

4. Results and Discussion

On 9 March, 2013, in Anpeng town, water samples from five groundwater inrush points and surrounding six water quality monitoring points (resident well) were tested, the result of water chemical composition are shown in Table 2, the distribution of sampling points is shown in Fig. 3.

According to the water quality analysis, the inrush brine had relatively high salinity, with some inrush water samples containing SO_4 Na and some containing HCO_3 Na. The crystals mainly consist of $NaSO_4$, Na_2CO_3, and $NaHCO_3$. The composition of inrush water and the crystals were the same as those of the high-concentrated ions in the trona brine (Na_2CO_3, $NaHCO_3$, etc.) and glauber salt brine (Na_2SO_4).

4.1. The source of inrush water

The automatic water quality recorder was set up at the Y5 inrush point on 4 March, 2013. The monitoring time lasted from 5 March to 20 March, 2013. Thus, the relationship between the inrush points and the S02 well can be judged according to the correlation of the changes between temperature/electrical conductivity and the concentration of brine during the S02 production well reparation period (5-14 March, 2013).

The production of glauber was stopped during the investigation (March 2-15, 2013), so it could be judged how serious glauber mining affects water inrush hazard based on the dynamic water quality situation.

249 *4.1.1. The source of inrush water in Y-5 point*

250   After the successful reparation of the S02 well, the conductivity and temperature of inrush water

251 decreased significantly. The CO_3^{2-} concentration remained at 0, the concentration of HCO_3^- decreased

252 to 500m , while the concentration of SO_4^{2-} increased to 600meq/L. Subsequently, the

253 concentrations of these three ions were in a state of dynamic balance. The analysis shows that the

254 source of inrush water in Y-5 point is closely related to the S02 trona well.

255   In order to ensure that whether the glauber brine exists in this point as part of inrush source,

256 further analysis had been performed. The depth of the well rupture was 234 m; gypsum deposit was

257 developed in this depth. While the leakage of trona brine flowed through the gypsum deposit,

258 reactions would happen as shown in Eqs. (7) and (8).

259   According to the ion milliequivalent concentration (Ca^{2+} 0.61meq/L; CO_3^{2-} 905.3meq/L; HCO_3^-

260 1332.94meq/L; Cl^- 107.43meq/L; SO_4^{2-} 267.89meq/L) of Y-5 point: the concentration of Ca^{2+} was

261 negligible compared with other main ions. Only the reaction between CO_3^{2-} and $CaSO_4$ had to be

262 taken into account because of the large number of CO_3^{2-}, fast flow speed, short contact time with

263 gypsum and high temperature. The reaction of CO_3^{2-} and $CaSO_4$ would take place at a ratio of 1:1

264 according to Ep. (7), and three types of inrush water sources could be assumed under this

265 precondition:

266   (1) Inrush water source only came from trona brine

267   The CO_3^{2-} and $CaSO_4$ in the brine reacted at a ratio of 1:1, and the concentration of SO_4^{2-} was

268   equal to the reacted γCO_3^{2-} content. Thus, the $\gamma CO_3^{2-}/\gamma HCO_3^-$ ratio in the trona brine was equal to the

269     $\gamma(CO_3^{2-}+SO_4^{2-})/\gamma HCO_3^-$ ratio in the inrush water. From this calculation, it could be seen that

270     $\gamma(CO_3^{2-}+SO_4^{2-})/\gamma HCO_3^-$ was equal to 0.88, while $\gamma CO_3^{2-}/\gamma HCO_3^-$ ranged between 0.86 and 1.26. The

271   content of $\gamma(CO_3^{2-}+SO_4^{2-})/\gamma HCO_3^-$ was similar to $\gamma CO_3^{2-}/\gamma HCO_3^-$, therefore, the source of inrush water

272   was exclusively trona brine.

273   (2) Inrush water source only came from glauber brine

274   The $\gamma SO_4^{2-}/\gamma HCO_3^-$ ratio in glauber brine was equal to 1237.8, while it was equal to 0.19 in inrush

275   water. Therefore, the assumption was incorrect because of the widely varying ratio.

276   (3) Inrush water source came from the mixed brine of glauber and trona

277   Assuming that the contribution ratio of the glauber brine was x and that of the trona brine was y. If

278   the assumption was true: $1237.8 \times X + (0.86{\sim}1.26) \times Y = 0.88$. This equation showed that when

279   the contribution ratio of the trona brine was equal to 1, the contribution ratio of the glauber brine was

280   equal to 1.6×10^{-5}, which was too small to ignore.

281   Thus, it could be confirmed that the water inrush source of Y-5 exclusively was the leakage trona

282   brine coming from the broken S02 well.

283   *4.1.2. The sources of inrush water in Y-4, Y-3, Y-2, Y-1 points*

284   The inrush water quantity and dynamic variation of the concentration of SO_4^{2-} and HCO_3^- at

285 Y1-Y4 points were not obvious when the S02 well was under repair and all glauber wells were shut

286 down (2-15 March). This result shows that the sources of these water inrush points were not due to the

287 underground mining activities of glauber brine or the rupture of the S02 well, but because of the brine

288 leakage coming from other trona wells.

289 *4.1.3. Component and mixed proportion of inrush water*

290 The PHREEQC simulation conditions were assumed as follow: (1) the trona brine did not mix

291 with shallow groundwater after flowing through the mineral layer; (2) the trona brine mixed with

292 shallow groundwater under the ratio of 1:2, 1:10, 1:100, 1:200, 1:500, 1:1000 and 1:5000 after

293 flowing through the mineral layer. The simulation results are shown in Table 3.

294 Table 3 shows that when the trona brine flowed through the stratum and shallow groundwater, the

295 concentrations of Na^+, Cl^- and SO_4^{2-} decreased while the concentration of HCO_3^- increased with the

296 increasing proportion of the shallow water. The concentration of Ca^{2+} decreased at first and then

297 increases.

298 The ion concentrations in Y-5, except for SO_4^{2-}, were similar to the ion concentrations in trona

299 brine. However, at the same time, the concentration of HCO_3^- was almost 0. When the trona brine

300 flowed through the layer, it would react rapidly and pour out of the ground directly because of the fast

301 speed of inrush water in Y-5. Meanwhile, the trona brine was not continuously provided in the

302 simulation. Thus, the concentration of HCO_3^- would be close to the concentration of trona brine in

303   reality. Therefore, the trona brine must be a great deal of rapid inrush, nearly not mixing with shallow

304   groundwater.

305   The PHREEQC simulation analysis result shows that: the water inrush source of Y-5 was nearly

306   all of the trona brine from the ruptured S02 well; the water inrush source of Y-3 was a mixture of trona

307   brine and groundwater under the ratio of 1:10~1:100, while the water inrush sources of Y-4, Y-2 and

308   Y-1 were a mixture of trona brine and groundwater under the ratio of 1:200.

309   ***4.2. The channel of inrush water***

310   *4.2.1. Reason for brine leakage*

311   Trona is produced by either single well or double/multiple well convection mining method, which

312   belongs to water soluble mining method (Lin, 1987). The main mining unit is consisting of salt cavity

313   and production well. Thus, the instability of salt cavity and the rupture of production well are the main

314   possible reasons for brine leakage.

315   (1) Analysis of the salt cavity stability

316   The possibility of salt cavity collapse: Trona mineral is distributed at the bottom of the second

317   member of the Hetaoyuan Formation and in the upper part of the third member of the Hetaoyuan

318   Formation, with dolomite strata developed in the roof and floor. The thick and hard surrounding rock

319   structure determines that the cavity produced by hydrofracture is hard to fill with large-scale fractured

320   channels and can remain intact and stable.

321   The development of roof fracture: When a mineral is under exploiting, the surrounding rock in the

322   cavity is under the pressure from the inner brine. This pressure is equal to the water injection pressure

323   plus the water column pressure in the production well. The water injection pressure of trona

324   production well is approximately 10-20 MPa, meanwhile the 1560.92-2929.53 m (mineral buried

325   depth) water column pressure is approximately 15.3-28.71 MPa. Thus, the biggest water pressure on

326   the surrounding rock in the cavity is 48.71 MPa. The main lithology of the surrounding rock is

327   dolomite which is 500 m in thickness and 142.66 MPa in compressive strength, this compressive

328   strength is 3 times that of the biggest water pressure. Therefore, large-scale fractures in the

329   surrounding rock of trona mineral is difficult to develop under the effect of sustain water pressure.

330   (2) Analysis of production well rupture

331   The phenomenon of brine leakage caused by S02 well rupture in Anpeng town indicates that

332   production well damage is an important reason for brine leakage. The depth of the S02 well rupture is

333   234 m underground, i.e., in the gypsum deposit, which is strongly hygroscopic. The pressure caused

334   by water swelling is approximately 0.15 MPa (Li and Zhou, 1996), which may damage the production

335   well and induce brine leakage. The high concentration of SO_4^{2-} (>250 mg/L) generated by reaction of

336   leakage brine and gypsum can also corrode the production well and lead to groundwater inrush.

337   *4.2.2. Analysis of water-conducting channel*

338   According to our analysis, the most probable reason for brine leakage in trona is the production

339   well rupture. The leaking brine will flow along the water-conducting channel into the shallow aquifer

340   and even pour out to the ground. However the geological structure in the mining area shows no

341   water-conducting fault development. Thus, the water-conducting channel, which the leakage brine

342   flows along, is probably fissure or artificial channel.

343   Structural fissure is the main type of fissure that appears in groundwater inrush hazard when using

344   solution mining method. The structural fissure is determined by maximum horizontal principal stress,

345   which is controlled by the tectonic stress field in the mining area. The connection direction of the S02

346   well and other water inrush points is NW-SE, which is the same as that of the structural fissure zone

347   development direction. This indicates that the main water-conducting channel in Anpeng town is

348   controlled by the structural fissure zone.

349   The inrush points in Anpeng town are all located at the abandoned gypsum exploitation wells,

350   which were not strictly closed. Thus, the high-pressure cavity water or leakage brine can flow along

351   the structural fissure zone; finally connect with these wells, and then pour out of the ground through

352   boreholes. Therefore, the abandoned gypsum exploitation wells are the main channels through which

353   shallow polluted groundwater gushed out of the ground, as shown in Fig. 4.

354   **5. Conclusions**

355   This study aimed at investigating the source and channel of inrush water in a multilayer rock salt

356   mine area. To achieve the set objectives, this study combined analysis of geological and

357 hydrogeological conditions, analysis of physical and chemical reaction principle of different brines,

358 PHREEQC simulation method, and analysis of geological and artificial reason on the conducting

359 channel where leakage brine flowed from the damage depth to the ground as the study methodology.

360   Long-term solution mining with high-pressure and -temperature water not only dissolves minerals

361 but also may cause rupture of strata and damage of production well, which usually results in brine

362 leakage or the inrush of groundwater. Geological and hydrogeological conditions are the basis which

363 determines the total risk of groundwater inrush hazard. Physical and chemical reaction principle

364 analysis of different brines and hydrogeochemical simulation of water-rock interaction in different

365 assumed conditions by PHREEQC simulation method can not only determine the exact source of

366 leakage brine but also identify the mixed proportion of inrush water while the leakage brine flows

367 through the mineral layer in different way. Besides geological reason, mining technic such as pressure

368 control of injection water, groundwater quality monitoring of exploitation wells may also determines

369 the risk of a groundwater inrush hazard in a multilayer rock salt mine area.

370 **Acknowledgements**

371   This work was partially supported by the Fundamental Research Funds for the Central

372 Universities, China University of Geosciences (Wuhan) [Grant Numbers: CUGL100219].

373 **Author Contributions**

374   Bin Zeng and Tingting Shi contributed to data analysis and manuscript writing; Zhihua Chen

375   proposed the main structure of this study; Liu Xiang and Muyi Yang designed and performed the

376   experiments; Shaopeng Xiang performed the PHREEQC simulation. All authors read and approved

377   the final manuscript.

378   **Conflicts of Interest**

379   The authors declare that they have no conflict of interest.

380

381 **References**

382   Bonetto, S., Fiorucci, A., Fornaro, M. and Vigna, B.: Subsidence hazards connected to quarrying

383   activities in a karst area: the case of the Moncalvo sinkhole event (Piedmont, NW Italy),

384   Estonian J. Earth Sci., 57, 125-134, 2008

385   Blachowski, J., Milczarek, W. and Stefaniak, P.: Deformation information system for facilitating

386   studies of mining-ground deformations, development, and applications, Nat. Hazards Earth

387   Syst. Sci., 14, 1677-1689, 2014

388   Clark, I. D. and Fritz, P.: Environmental isotopes in hydrogeology, Lewis Publishers, New York,

389   USA, 35-37, 1997.

390   Chen, H. J. and Li, X. Bi.: Studies of water source determination method of mine water inrush

391   based on Bayes' multi-group stepwise discriminant analysis theory, Rock and Soil

392   Mechanics., 30, 3655-3659, 2009.

393   Closson, D. and Abou Karaki, N.: Salt karst and tectonics: sinkholes development along tension

394   cracks between parallel strike-slip faults , Dead Sea , Jordan. Earth Surface Processes and

395   Landforms., 1408-1421, 2009

396   Cobbina, S.J., Duwiejuah, A.B., Quansah, R., Obiri, S. and Bakobie, Noel.: Comparative

397   Assessment of Heavy Metals in Drinking Water Sources in Two Small-Scale Mining

398   Communities in Northern Ghana, Int. J. Environ. Res. Public Health., 12, 10620-10634,

399   2015.

400   Ezersky, M., Legchenko, A., Camerlynck, C. and Al-Zoubi, A.: Identification of sinkhole

401   development mechanism based on a combined geophysical study in Nahal Hever South area

402   (Dead Sea coast of Israel). Environmental Geology., 58, 1123-1141, 2009

403   Ezersky, M. and Frumkin, A.: Fault - Dissolution front relations and the Dead Sea sinkhole

404   problem. Geomorphology., 201, 35-44, 2013

405   Fernandez, I., Olias, M., Ceron, J.C. and De la Rosa, J.: Application of lead stable isotopes to the

406   Guadiamar Aquifer study after the mine tailings spill in Aznalcollar (SW Spain), Environ

407   Geol., 47, 197-204, 2005.

408   Fernandez-Galvez, J., Barahona, E., Iriarte, A. and Mingorance, M.D.: A simple methodology for

409   the evaluation of groundwater pollution risks, Sci Total Environ**.,** 378, 67-70, 2007.

410   Frumkin, A., Ezersky, M., Al-Zoubi, A., Akkawi, E. and Abueladas, A.-R.: The Dead Sea

411   sinkhole hazard: Geophysical assessment of salt dissolution and collapse. Geomorphology.,

412   134, 102-117, 2011

413   Goldscheider, N. and Bechtel, T.D.: The housing crises from underground – damage to a historic

414   town by geothermal drillings through anhydrite, Staufen, Germany. Hydrogeology Journal.,

415   17, 491-493, 2009

416   Gao, W.D.: Application of Entropy Fuzzy Discriminating methods in Distinguishing Mine

417   Bursting Water Source, Mining Safety & Environmental Protection., 39, 22-24, 2012.

418   Gutierrez, F., Parise, M., De, Waele, J. and Jourde, H.: A review on natural and human-induced

419   geohazards and impacts in karst. Earth Science Reviews., 138, 61-88, 2014

420   Hao, B.B., Li C. and Wang C.H.: Application of grey correlation degree in the identification of

421   sources of mine water bursting, China Coal., 36, 20-22, 2010.

422   Hu, W.W., Ma, Z.Y., Cao, H.D., Liu, F., Li, T. and Dou, H.P.: Application of Isotope and

423   Hydrogeochemical Methods in Distinguishing Mine Bursting Water Source, Journal of Earth

424   Sciences and Environment., 32, 268-271, 2010.

425   Houben, G.J., Sitnikova, M.A. and Post, V.E.A.: Terrestrial sedimentary pyrites as a potential

426   source of trace metal release to groundwater – A case study from the Emsland, Germany,

427   Appl. Geochem., 76, 99-111, 2017.

428   Jiang, R.Z. and Jiang T.X.: Present Development and Prospecting of Hydraulic Fracturing

429   Technology, Oil Drilling & Production Technology., 26, 52-57, 2004.

430   Kotwica, K.: Scenarios of technological development of roadwavs mining in polish coal mines

431   conditions, Gospod Surowcami Min., 24, 139-152, 2008.

432   Kang, X.B., Hu, X.W. and Xie, H.Q.: Numerical simulation on the influence of the groundwater

433   flow field during tunneling, Advanced Materials Research., pp. 1230-1233, 2012.

434   Lin, Y.X.: The History of Science & Technology of well salt in China, Sichuan Science and

435   Technology Pres, Chengdu, 1987.

436   Li, D.D. and Zhou, Z.A.: Possibility of corrosion failure of concrete shaftwall due to water

437   infiltration, Journal of China Coal Society., 21, 158-163, 1996.

438   Liu, H., Yang, T., Zhu, W. and Yu, Q.: Numerical analysis of the process of water inrush from the

439   12th coal floor FANGEZHUANG coal mine in China, Controlling Seismic Hazard and

440   Sustainable Development of Deep Mines: 7th International Symposium on ROCKBURST

441   and Seismicity in Mines (RASIM7)., 1&2, 1381-1386, 2009.

442   Lu, J.T.: Recognizing of Mine Water Inrush Sources Based on Principal Components Analysis

443   and Fisher Discrimination Analysis Method, China Safety Science Journal., 22, 109-115,

444   2012.

445   Lollino, P., Martimucci, V. and Parise, M.: Geological survey and numerical modeling of the

446   potential failure mechanisms of underground caves. Geosystem Engineering., 16,   100-112,

447   2013

448   Liu, R.Z., Liu, J., Zhang, Z.J., Borthwick, A. and Zhang, K.: Accidental Water Pollution Risk

449   Analysis of Mine Tailings Ponds in Guanting Reservoir Watershed, Zhangjiakou City, China,

450   Int. J. Environ. Res. Public Health., 12, 15269-15284, 2015.

451   Lee, H., Choi, Y., Suh, J. and Lee, S.H.: Mapping Copper and Lead Concentrations at Abandoned

452   Mine Areas Using Element Analysis Data from ICP–AES and Portable XRF Instruments: A

453   Comparative Study, Int. J. Environ. Res. Public Health., 13, 384, 2016.

454   LeDoux, T.M., Szynkiewicz, A. and Faiia, A.M.: Chemical and isotope compositions of

455   shallowgroundwater in areas impacted by hydraulic fracturing and surface mining in the

456   Central Appalachian Basin, Eastern United States, Appl. Geochem., 71, 73-85, 2016.

457   Ma, L. and Qian, J.Z.: An approach for quickly identifying water-inrush source of mine based on

458   GIS and groundwater chemistry and temperature, Coal Geology & Exploration., 42, 49-53,

459   2014.

460   Namin, F. S., Shahriar K., Bascetin A. and Ghodsypour S.H.: Practical applications from

461   decision-making techniques for selection of suitable mining method in Iran, Gospod

462   Surowcami Min., 25, 57-77, 2009.

463   Parise, M., and Gunn, J.: Natural and anthropogenic hazards in karst areas: Recognition, Analysis

464   and Mitigation. Geol. Soc. London, sp. publ. 279, 2007

465   Parise, M. and Lollino, P.: A preliminary analysis of failure mechanisms in karst and man-made

466   underground caves in Southern Italy. Geomorphology., 134, 132-143, 2011

467   Parise, M., Closson, D., Gutierrez, F. and Stevanovic, Z.: Anticipating and managing engineering

468   problems in the complex karst environment. Environmental Earth Sciences., 74, 7823-7835,

469   DOI :10.1007/s12665-015-4647-5, 2015

470   Qiu, Z.Y.: Mechanism analysis of surface collapse in the area of solution salt mining, Journal of

471   Safety Science and Technology., 7, 27-31, 2011.

472   Robins, N.S.: Groundwater quality in Scotland: major ion chemistry of the key groundwater

473   bodies, Sci Total Environ., 294, 41-56, 2002.

474   Ramadas, M., Ojha, R. and Govindaraju, R.S.: Current and Future Challenges in Groundwater. II:

475   Water Quality Modeling, J. Hydrol. Eng., 13, 132-140, 2015.

476   Staudtmeister, K. and Rokahr, R.B.: Rock Mechanical Design of Storage Caverns For Natural

477   Gas in Rock Salt Mass, Rock Mech&Min.Sci., 34, 3-4, 1997.

478   Shao, A.J., Huang, Y. and Meng, Q.X.: Numerical Simulation on Water Invasion of Coal Mine,

479   Applied Mechanics and Materials., pp. 1112-1117, 2013.

480   Shi, T.T., Chen, Z.H. and Luo, Z.H.: Mechanism of groundwater bursting in a deep rock salt mine

481   region: a case study of the Anpeng trona and glauber salt mines, China, Environ Earth Sci.,

482   68, 229-239, 2013.

483   Vigna, B., Fiorucci, A., Banzato, C., Forti, P. and De Waele, J.: Hypogene gypsum karst and

484   sinkhole formation at Moncalvo (Asti, Italy). Z. Geomorphol., 54, 285-308, 2010

485   Wang, J.M.: A Preliminary Study on the Characteristics and Conditions of forming Anpeng Trona

486   deposits, Petrol Explor Dev., 5, 93-99, 1987.

487   Waltham, AC. And Fookes, PG.: Engineering classification of karst ground conditions. Quarterly

488   Journal of Engineering Geology and Hydrogeology., 36, 101-118, 2003

489   Wei, Y.N.: Research and Application of Hydro-geochemical Simulation, Journal of Water

490   Resources and Water Engineering., 21, 58-61, 2010.

491   Wu, Q., Li, B. and Chen, Y.: Vulnerability Assessment of Groundwater Inrush from Underlying

492   Aquifers Based on Variable Weight Model and its Application, Water Resour Manag., 30,

493   3331-3345, 2016.

494   Xu, H. and Li, H.S.: Study on $CaSO_4$ crystallization process and its influential factors, Industrial

495   Water Treatment., 5, 67-69, 2011.

496   Yang, Y.H.: Gypsum mineral dissolution kinetics, M.D. thesis, China University of Geosciences,

497   Wuhan, China, 2003.

498   Yuan, W.H. and Gui, H.R.: The Characteristics of Geothermal Temperature and Its Application in

499   Distinguishing the Source of Water in Ren Lou Mine, Journal of Anhui University of Science

500   and Technology (Natural Science)., 25, 9-11, 2005.

501   Zhou, W. and Beck, BF.: Engineering issues on karst. In: P. van Beynen (Ed), Karst Management.

502   Springer, Dordrecht, pp. 9-45, 2011

Figure captions

Fig. 1. One of the long-term (more than 2 years) groundwater inrush points with stable discharge (Y-3).

Fig. 2. The sudden groundwater inrush point (Y-5). As shown in this figure, the high-temperature inrush groundwater was being pumped after the ground was broken.

Fig. 3. Information about strata, lithology, aquifer, and buried position of each ore bed in the mining area.

Fig. 4. Sketch map of hydrogeological conditions and distribution of groundwater inrush points in mining area.

Fig. 5. Schematic diagram of source and channel analysis of groundwater inrush hazard in the multilayer rock salt mine area in Tongbai County.

Fig.1

Fig.2
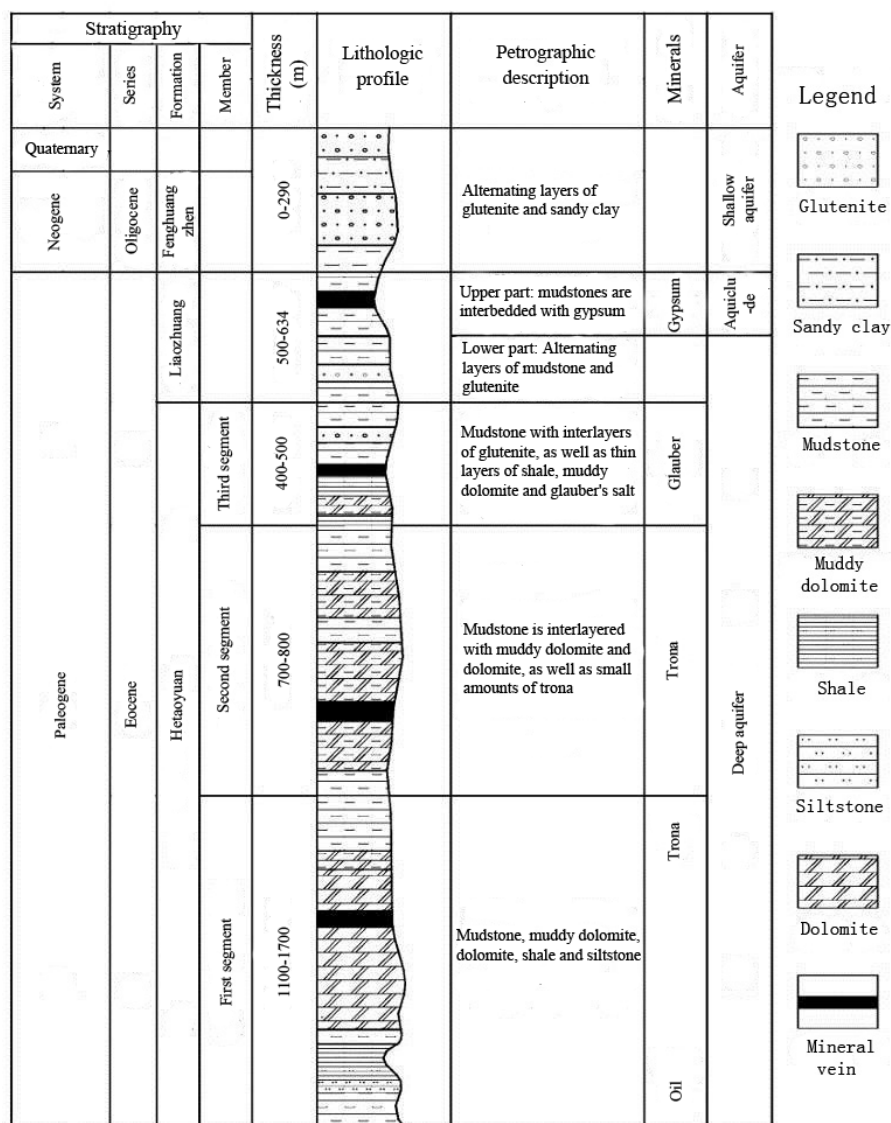
Fig.3
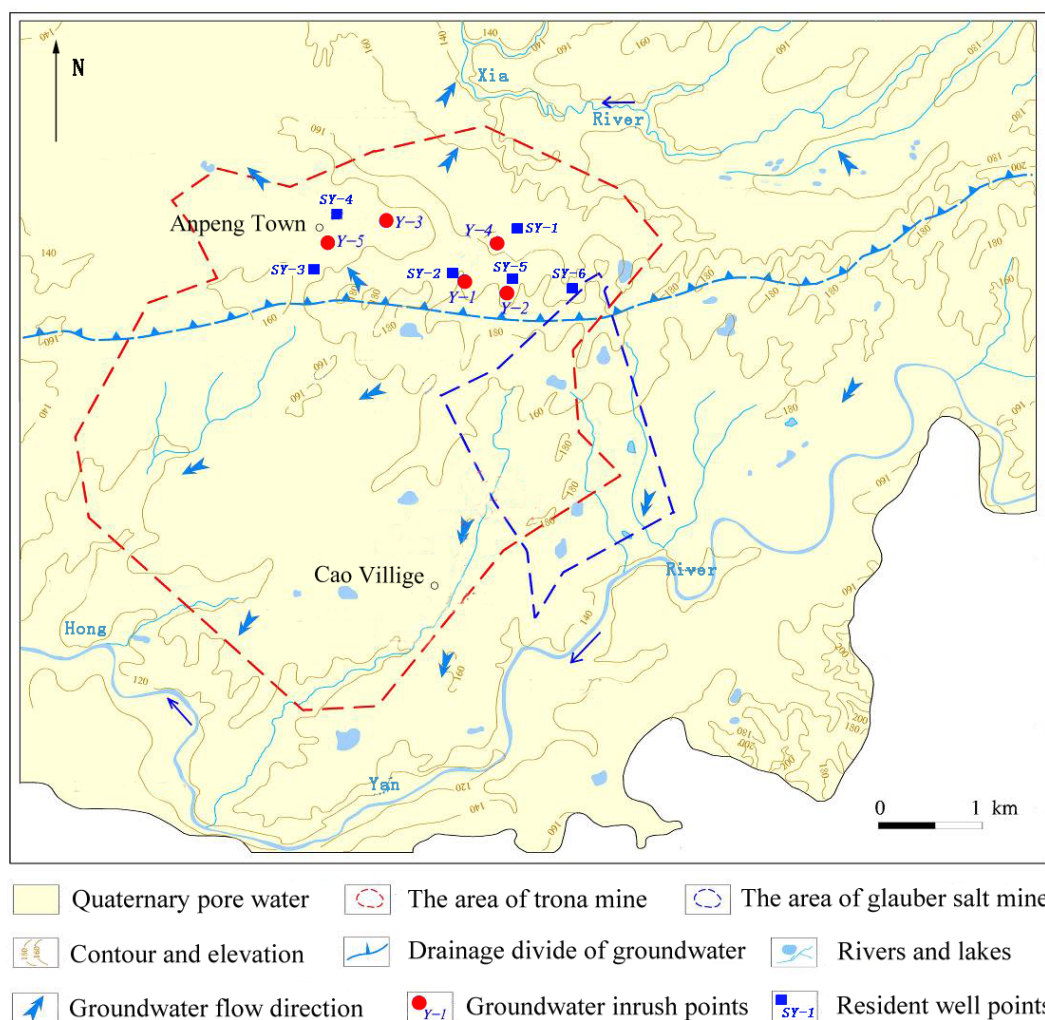
Fig.4
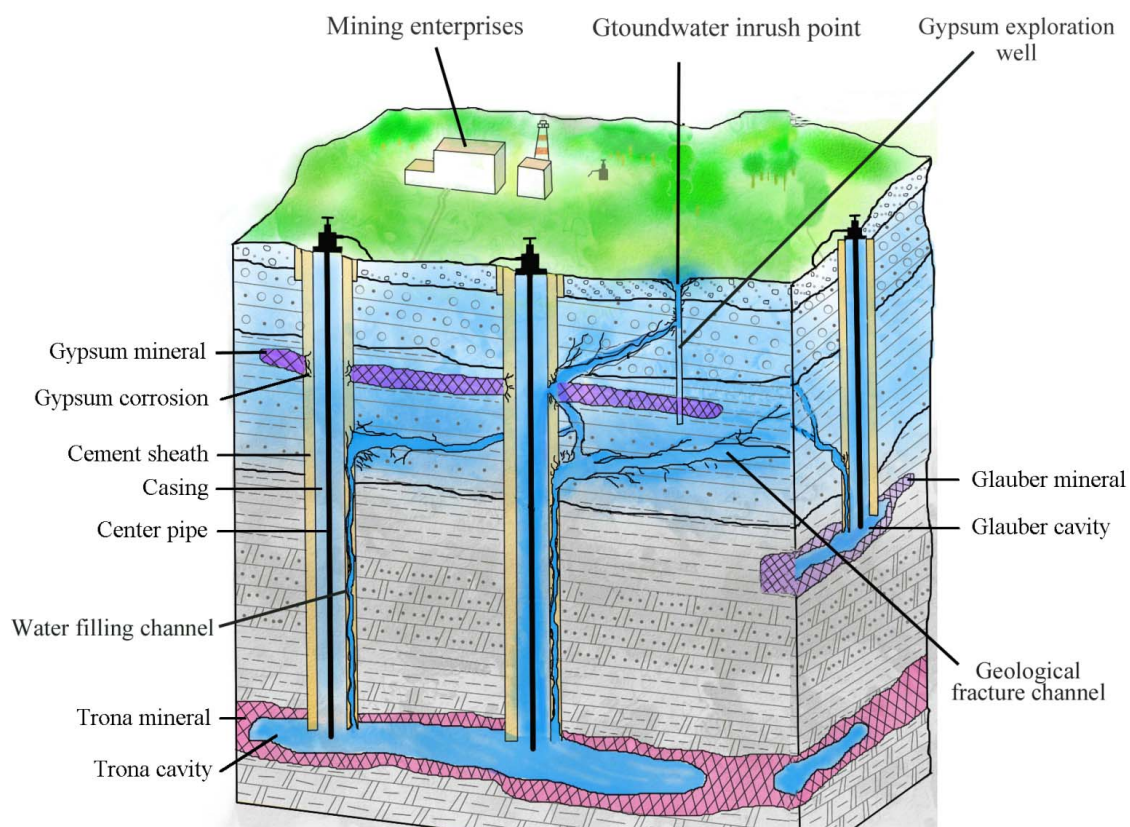
Fig.5

Table 1 Initial data of trona brine and background value of groundwater for PHREEQC simulation

Type	Temperature (°C)	pH	Na$^+$	Ca^{2+}	Mg^{2+}	Cl$^-$ (mg/L)	SO$_4{}^{2-}$	HCO$_3{}^-$	CO$_3{}^{2-}$
Trona brine	70.0	10.8	85880	5.0	1.0	3819	206.0	104721	4565
Background value of groundwater	14.1	7.5	38.76	67.10	23.88	12.46	39.31	386.87	0.00

Table 2 Chemical composition of groundwater from inrush hazard points and surrounding resident wells

Source	Point	Na^+	Ca^{2+}	Mg^{2+}	Cl^-	SO_4^{2-}	HCO_3^-	CO_3^{2-}	Salinity	Depth
						(mg/L)				(m)
Groundwater from inrush hazard points	Y-1	447.30	91.2	74.68	171.18	278.55	1488.89	0.00	1807.35	
	Y-2	524.50	89.34	75.32	153.97	298.88	1525.00	0.00	1904.51	330.55 ~ 430.2
	Y-3	1132.00	146.6	158.30	125.56	4296.44	1012.93	0.00	6365.37	
	Y-4	322.12	98.67	123.88	210.78	346.55	1122.77	0.00	1663.38	
	Y-5	50300.00	12.23	53.21	3813.80	12858.63	81309.15	27159.0	107692.4	
Groundwater from resident wells around the inrush points	SY-1	46.28	76.76	17.29	64.3	14.58	319.03	0.00	378.73	
	SY-2	28.37	98.02	27.46	26.16	10.38	453.84	0.00	417.31	
	SY-3	43.14	46.2	14.42	31.02	117.12	319.03	0.00	316.26	10.00
	SY-4	118.53	278.4	72.3	425.23	175.96	568.52	0.00	1354.68	
	SY-5	31.67	95.51	19.22	53.93	22.59	351.97	0.00	398.9	
	SY-6	36.77	68.82	19.6	18.51	21.55	340.38	0.00	335.43	

Table 3 Simulation results for mixed proportion of inrush trona brine by PHREEQC (mg/L)

Conditions	Mixed proportion with shallow groundwater	Na^+	Ca^{2+}	Cl^-	SO_4^{2-}	HCO_3^-
	Unmixing	87147.00	301.08	3880.15	68659.20	5.06
Trona brine unmixed or mixed with different proportion of shallow groundwater after flowing through the mineral layer (simulation results)	1:1	48093.00	280.00	2145.62	37900.80	9.39
	1:2	33235.00	184.72	1485.68	26188.80	13.97
	1:10	9586.40	148.28	436.30	7561.92	57.95
	1:100	1098.25	90.40	141.63	873.89	306.34
	1:200	571.78	69.60	118.56	459.17	382.17
	1:500	252.77	68.32	104.60	207.84	453.66
	1:1000	144.81	67.52	99.94	105.12	481.60
Water quality test results in five water inrush hazard points	Y-1	447.30	91.20	171.18	276.55	1488.89
	Y-2	524.50	89.34	153.97	298.88	1525.00
	Y-3	1132.00	146.60	125.56	4296.44	1012.93
	Y-4	322.12	98.67	210.78	346.55	1122.77
	Y-5	50300.00	12.23	3813.80	12858.63	81309.15